J. Ocean Univ. China (Oceanic and Coastal Sea Research)
https://doi.org/10.1007/s11802-022-4695-x
ISSN 1672-5182, 2022 21 (1): 69-80
http://www.ouc.edu.cn/xbywb/
E-mail:xbywb@ouc.edu.cn

Variations of the Eco-Hydro-Climatic Environment Response to the 2015/2016 Super El Niño Event in the Mindanao Dome Upwelling System

GAO Wei[1)], WANG Zhenyan[1), 2), 3), 4), *], and HUANG Haijun[1), 3), 4)]

1) *CAS Key Laboratory of Marine Geology and Environment*, *Institute of Oceanology*, *Chinese Academy of Sciences*, *Qingdao* 266071, *China*
2) *Laboratory for Marine Mineral Resources*, *Pilot National Laboratory for Marine Science and Technology*, *Qingdao* 266071, *China*
3) *Center for Ocean Mega-Science*, *Chinese Academy of Sciences*, *Qingdao* 266071, *China*
4) *University of Chinese Academy of Sciences*, *Beijing* 100049, *China*

(Received July 30, 2020; revised September 25, 2020; accepted November 3, 2021)

Abstract A super El Niño event occurred in the equatorial Pacific during 2015–2016, accompanied by considerable regional eco-hydro-climatic variations within the Mindanao Dome (MD) upwelling system in the tropical western Pacific. Using timeseries of various oceanic data from 2013 to 2017, the variability of eco-hydro-climatic conditions response to the 2015/2016 super El Niño in the upper 300 m of the MD region are analyzed in this paper. Results showed that during the 2015/2016 super El Niño event, the upwelling in the MD region was greatly enhanced compared to those before and after this El Niño event. Upwelling Rossby waves and the massive loss of surface water in the western Pacific were suggested to be the main reasons for this enhanced upwelling. Decreased precipitation caused by changes in large-scale air-sea interaction led to the increased surface salinities. Changes in the structures of the thermohaline and nutrient distribution in deep waters contributed to the increased surface chlorophyll *a*, suggesting a positive effect of El Niño on surface carbon storage in the MD region. Based on the above analysis, the synopsis mechanism illustrating the eco-hydro-climatic changing processes over the MD upwelling system responding to the El Niño event was proposed. It highlights the prospect for the role played by El Niño in local eco-hydro-climatic effects, which has further profound implications for understanding the influence of the global climate changes on the ocean carbon cycle.

Key words Mindanao Dome region; upwelling; eco-hydro-climatic variations; 2015/2016 super El Niño event; carbon cycle

1 Introduction

There are several large-scale thermal upwelling domes in the world oceans, which are accompanied by the intense advection of different water masses and their vertical and horizontal mixing. The movement of water from deeper layers to the surface not only is pivotal to the exchange of heat between the air and sea but also has a significant influence on the hydrochemical structure and biological activities (Sydeman *et al*., 2014). Hence, understanding the physical processes of upwelling and its variability is crucial for monitoring the local oceanic ecosystem, thermohaline circulation and climate.

One of those located in the tropical western Pacific with a near-surface, wind-driven cyclonic gyre on the east of Mindanao Island (Tozuka *et al*., 2002; Suzuki *et al*., 2005) (Fig.1) has been recognized for over half a century; this area was first named the Mindanao Dome (MD) by Masumoto and Yamagata (1991). This upwelling structure can be distinguished by its abnormal cold temperature at the subsurface layer rather than sea surface (Udarbe-Walker and Villanoy, 2001).

The study area, where the MD developed, is a 'crossroad' not only for the water masses but also for the ocean currents in the tropical western Pacific (Rothstein *et al*., 1998; Kashino *et al*., 2011), which connects with the subtropical gyre through North Equatorial Current (NEC) and the equatorial region by North Equatorial Counter Current (NECC), playing important roles in the heat budge of the West Pacific Warm Pool (WPWP) and in global ocean circulation (Zhao *et al*., 2013; Hu *et al*., 2015). In addition, the upwelling in the MD region creates the large-scale water movement from deeper layers to the surface, which is pivotal to the exchange of heat between the air and sea and has a significant influence on the hydrochemical structure and ecosystems (Lengaigne *et al*., 2007; Gruber *et al*., 2011; Sydeman *et al*., 2014). What's more, it is well known that variations in heat contents and circulation

* Corresponding author. Tel: 0086-532-82898539
E-mail: zywang@qdio.ac.cn

of WPWP not only exhibit a response to El Niño-Southern Oscillation (ENSO) but also induce a feedback onto El Niño (Cravatte *et al*., 2009; Izumo *et al*., 2010; Zhang *et al*., 2018, 2019). However, the relationship between ENSO and the oceanic variations in the MD upwelling system, which locates in the western deep part of WPWP, is still seldom systematically discussed.

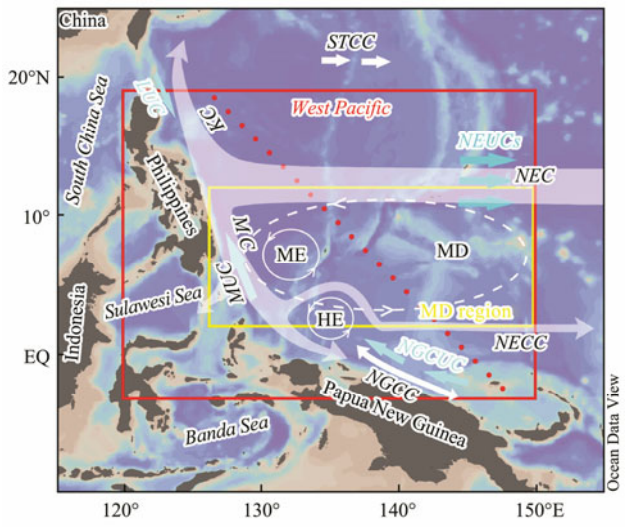

Fig.1 Map of the western Pacific showing the bathymetry, the current system, the location of study area (red rectangle: 5°S – 20°N, 120° – 150°E) and the zone of the Mindanao Dome (MD) upwelling system (yellow rectangle: 2° – 12°N, 125° – 150°E). NEC, North Equatorial Current; MC, Mindanao Current; KC, Kuroshio Current; NECC, North Equatorial Counter Current; NGCC, New Guinea Coastal Current; STCC, North Pacific Subtropical Countercurrent; ME, Mindanao Eddy; HE, Halmahera Eddy; MD, Mindanao Dome; MUC, Mindanao Undercurrent; LUC, Luzon Undercurrent; NEUC, North Equatorial Undercurrent; NGCUC, New Guinea Counter Undercurrent.

Recently, the mechanisms responsible for the variations of the upwelling system at seasonal to interannual scales in the MD region have been demonstrated by using different models (*e.g*., Suzuki *et al*., 2005, Kashino *et al*., 2011; Chen *et al*., 2015). The local Ekman upwelling induced by the positive wind stress curl during the northeast Asian winter monsoon has been proposed to be the key factor influencing the formation of the MD, while the warm anomaly that propagates from the eastern tropical Pacific plays an important role in its attenuation (Tozuka *et al*., 2002; Suzuki *et al*., 2005). Yet, few studies have been conducted on the thermohaline structural variations exhibited by the upwelling in the MD region during El Niño event. The relationship between the variations in the upwelling process within the MD region and the local hydroclimatic conditions during El Niño event need be further established. This constitutes one of the main motives of the present study. This work was conceived to characterize and illustrate the variations in the three-dimensional thermohaline structure of the upwelling system in the MD region during the 2015/2016 super El Niño event and to examine the role of those variations in changing the local ecosystem and hydroclimate.

2 Data and Methods

2.1 Data

In this paper, we choose the upper 300 m of the region bounded by 5°S – 20°N and 120° – 150°E as the study area, delineated by the red rectangle in Fig.1, to investigate the oceanic variations within the upper MD region. Considering the 2015/2016 super El Niño event peaked in late fall to early winter (Iskandar *et al*., 2017; Santoso *et al*., 2017), we chose December as the typical month and analyzed a series of oceanic parameters in the MD region for each December during 2013 – 2017, especially focusing on the abnormal oceanic features in the tropical western Pacific associated with this super El Niño event.

Various oceanic fields are utilized herein to illustrate the oceanic variations caused by the 2015/2016 super El Niño event. The gridded temperature and salinity data used in this paper were derived from Argo products provided by the International Pacific Research Center (IPRC)/Asia-Pacific Data-Research Center (APDRC); these data are composed of monthly mean fields spatially averaged at a 1° horizontal resolution at standard depths (0 m, 50 m, 100 m, 150 m, 200 m, and 300 m). The Argo-based profile S, shown as the red dots in Fig.1, was selected to display the vertical thermohaline structure in the study area.

Data of the surface currents, heat contents (0 – 300 m) and surface Chl-*a* concentrations and Wind Stress Curl (WSC) were developed from the Surface Currents from Diagnostic (SCUD) model, Climate Forecast System version 2 model, Moderate Resolution Imaging Spectroradiometer (MODIS) Aqua satellite and the Ifremer satellite products, respectively. The surface current data have a 0.25°×0.25° spatial resolution with a 1-day interval, while the heat content data have a 0.5°×0.5° spatial resolution with a 1-day interval but data in December 2017 are missing. The surface Chl-*a* concentration data have a 0.5°×0.5° spatial resolution with a 1-month interval. And the WSC data have a 0.25°× 0.25° spatial resolution with a 6-hour interval. All these data are obtained from the IPRC/APDRC public servers and are available online at http://apdrc.soest.hawaii.edu.

The altimeter products of the multi-mission gridded mean sea level anomaly (MSLA) data used in this paper were extracted from the National Oceanic and Atmospheric Administration (NOAA) Ocean Watch Dataset (http://oceanwatch.pifsc.noaa.gov/) with a 0.25°×0.25° spatial resolution for the entire sampling period. In addition, merged AVISO products were downloaded as global delayed-time data files with a 7-day interval for each December during 2013 – 2016 and as near-real-time data files with a 1-day interval for December 2017.

The precipitation products used in this study are high spatial resolution (0.25°×0.25°) gridded monthly data, which were obtained from the Climate Prediction Center (CPC) Merged Analysis of Precipitation (CMAP) (https://www.esrl.noaa.gov/psd/data). Since the CMAP data were derived by merging multisource estimates, including gauge obser-

vations, five different satellite estimates, and numerical model outputs, the uncertainties contained in each individual estimate are significantly reduced.

2.2 Data Processing

All original data were first averaged from daily/weekly intervals into monthly mean data. A typical zone (2°–12°N, 125°–150°E) was selected to represent the upwelling zone of the MD region (represented by the yellow rectangle in Fig.1). Then, the Argo-based temperature and salinity data at each standard depth in the selected upwelling zone were calculated and averaged for further detailed analysis and discussion. In addition, the MSLA, heat content, precipitation, surface Chl-*a* concentration and WSC data in this selected zone were extracted and averaged. All the processed data were plotted by using professional drawing software, including Ocean Data View 4, Grapher 9, and Corel-Draw X7.

3 Results

3.1 Variations in the Thermohaline Structure of the Upwelling in the MD Region

To investigate the thermohaline structural variations of the upwelling in the MD region related to the 2015/2016 super El Niño event, we recreated the thermohaline structure of the study area in December 2013–2017 using the combination of plan and selected profile plots (Figs.2 and 3).

3.1.1 Vertical thermohaline distribution

The temperature and salinity profiles (Figs.2 and 3g-1 to

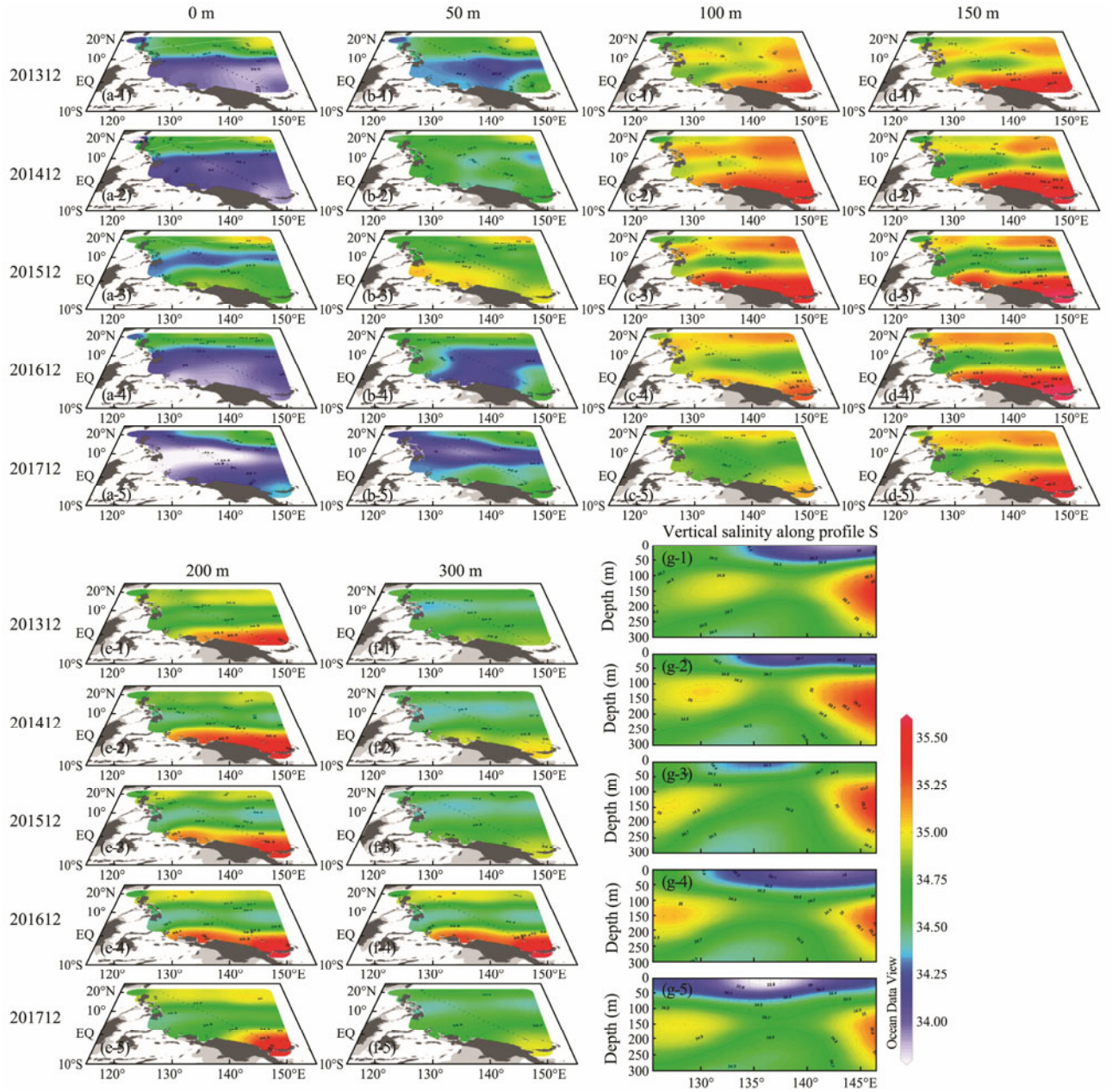

Fig.2 Monthly mean temperature distributions at six standard depths (0 m, 50 m, 100 m, 150 m, 200 m, and 300 m) (a-1 to f-5, successively) and selected profile plots (g-1 to g-5) above 300 m in December 2013–2017 in the Mindanao Dome region. The black dotted lines in a–f indicate the position of the selected profiles diagnosed from Argo products.

g-5, respectively) reveal that the upwelling feature was ubiquitous in the study area, which is typical of the MD. Furthermore, the water column in the study area was occupied by different water masses. The waters in the surface layer were mixed well and characterized by relatively high temperatures (>28℃) but notably low salinities (<34.6); here, we call this water mass as the North Pacific Surface Water (NPSW). However, the thickness of this surface water was relatively small, and in December 2015 its temperature and salinity were lower and higher, respectively, than those in the other four years.

In the subsurface layer, the shallow waters were occupied by two relatively high-salinity water masses located to the northwest and southeast of the selected profile. The mass to the northwest, which showed relatively low center salinities (35.0−35.1), is recognized as the North Pacific Tropical Water (NPTW, Suga *et al*., 2000). The other one to the southeast, which presented relatively high center salinities (>35.3), is known as the South Pacific Tropical Water (SPTW, O'Connor *et al*., 2002). The upwelling in the MD region seemed to truncate these two high-salinity water masses and transported deep cold and low-salinity water (North Pacific Intermediate Water, NPIW, Talley, 1993) upward, though this water did not reach the sea surface. In particular, the upwelling was greatly reinforced in December 2015, during which the deep NPIW was carried up to a much shallower depth, which obviously restricted the volumes of the shallower NPSW, NPTW and SPTW.

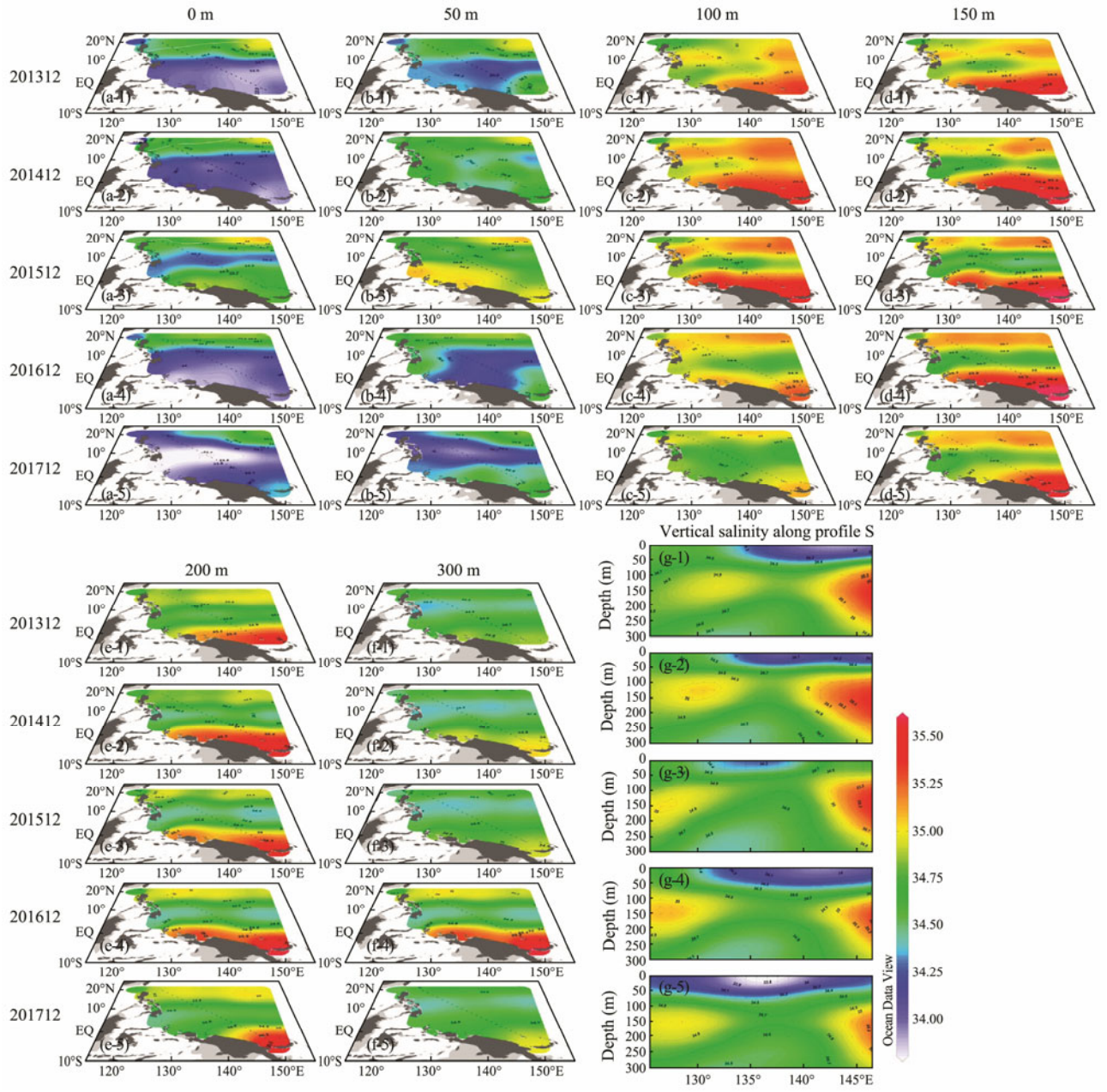

Fig.3 Monthly mean salinity distributions at six standard depths (0 m, 50 m, 100 m, 150 m, 200 m, and 300 m) (a-1 to f-5, successively) and selected profile plots (g-1 to g-5) above 300 m in December 2013−2017 in the Mindanao Dome region. The black dotted lines in a−f indicate the position of the selected profiles diagnosed from Argo products.

3.1.2 Horizontal thermohaline distribution

As shown in the plans in Figs.2 and 3, the cold and hypohaline anomalies caused by the upwelling appeared prevalently in the subsurface layer on the east of Mindanao in all five years and extended eastward like a band with increasing depth. In December 2013, 2014, 2016, and 2017, these anomalies can be discovered at approximately 100 m (Figs.2 and 3c-1, c-2, c-4, and c-5); additionally, the anomaly centers were close to the coast of Mindanao. However, the cold and hypohaline anomaly signals appeared even in the 50 m layer (Fig.2b-3) owing to the enhanced upwelling in December 2015. Nevertheless, it should be noted that this upwelling water possibly appeared at even shallower depths, which were not analyzed in this work that is only limited to the standard depths. Moreover, the locations of the temperature and salinity anomalies evidently moved eastward in 2015 relative to the other four years.

In addition, at the surface and 50 m layer, the salinity distribution exhibited more complex features than the temperature distribution in December 2015 relative to the other four years. At the surface, the sea surface salinity (SSS) showed almost the same distribution pattern in December 2013, 2014, 2016, and 2017. Relatively high SSS values (> 34.5) were found to the far north/northeast, while broad tracts of low SSS values (<34.0) occurred in the central and southern parts of the study area (Figs.3a-1, a-2, a-4, and a-5). However, in December 2015, low SSS values occurred at the surface, although the lowest value increased slightly, and the area of these low values shrank considerably, forming only a narrow belt along 10°N (Fig.3a-3). In contrast, the regions to the north and especially the south of this low-salinity belt were occupied by relatively high-salinity waters. Furthermore, in the 50 m layer, a large body of relatively high-salinity water appeared to the east of Mindanao Island.

3.2 Related Hydroclimatic Variations in the MD Region

3.2.1 Surface currents

In December 2013–2017, the surface NEC-Kuroshio Current (KC)-MC-NECC system (Hu *et al*., 2015) was present as a permanent feature (Figs.4a–e). The surface currents in the MD region formed a large-scale anticlockwise circulation, *i.e*., the Mindanao Eddy, which was generally centered near Mindanao Island. It is worth noting that in December 2015, the area of this anticlockwise circulation in the MD region became slightly enlarged, and the eastward-flowing NECC clearly strengthened. Moreover, another robust anticlockwise circulation developed to the east of the Mindanao Eddy.

3.2.2 Sea level anomaly

The monthly MSLA distributions shown in Figs.5a–e in December 2013–2017 exhibited different features. In December 2013, most of the study area was dominated by the positive MSLA, except for the northernmost part, where several areas with the negative MSLA existed. In December 2014, the slightly negative MSLA area in the north expanded southward, while the positive MSLA area shrank southward; additionally, several negative MSLA centers (<−0.20 m) and positive MSLA centers (>0.05 m) were interspersed in the north. In December 2015, the MSLA showed the distribution trend almost opposite to that in December 2013. The central and southern parts of the study area exhibited the negative MSLA overall, including three different yet notable negative centers (<−0.35 m) in the central-west part, while the northernmost extent of the study area presented the obviously positive MSLA. In December

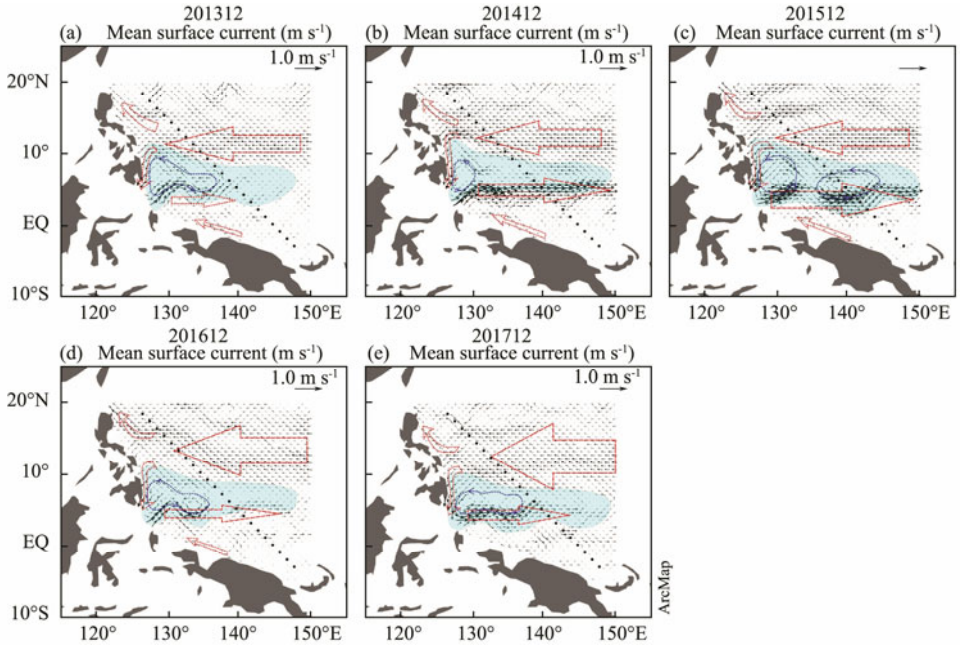

Fig.4 The distributions of the mean surface currents in December 2013–2017. The sky blue area represents the Mindanao Dome region, the red arrows represent the main surface currents, and the blue circles represent the anticlockwise centers in the Mindanao Dome region.

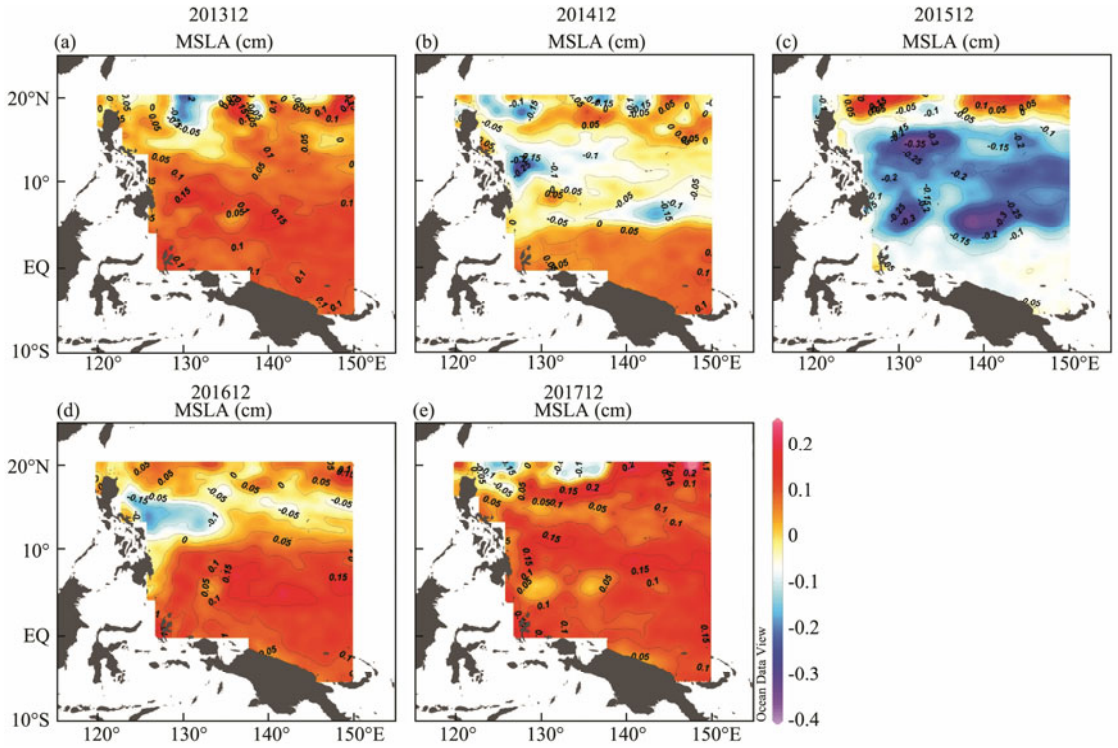

Fig.5 The distributions of the mean sea level anomaly (MSLA) in December 2013–2017.

2016 and 2017, the MSLA trends same as December 2013 appeared again; however, the negative MSLA extended southward slightly in December 2016.

3.2.3 Heat content

The monthly mean heat content distributions throughout the study area in December 2013–2016 demonstrated a layered zonal structure (Figs.6a–e; there were no data in December 2017). There was always a band exhibiting a low heat content between 5°N and 15°N, which was compressed between two bands of high heat. However, the spatial scale and heat content range of this low-heat-content band in December of these four years exhibited substantial differences. In December 2013 and 2016, the band with low heat contents is characterized by a small low-heat-content

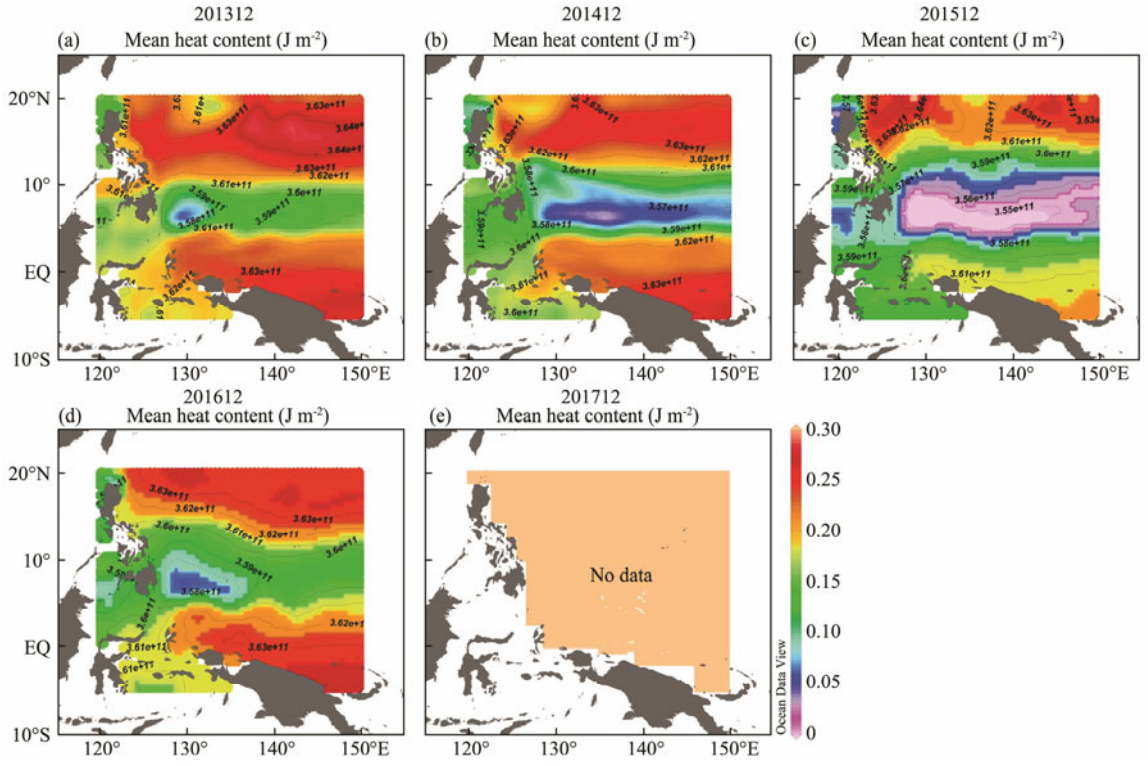

Fig.6 The distributions of the mean heat contents (0–300 m) in December 2013 – 2017.

center off the coast of Mindanao Island. In December 2014, the low-heat-content zone extended eastward resembling a band, and the heat content values decreased sharply. Subsequently, this trend was further reinforced in December 2015, when the low-heat-content zone extended eastward and covered the whole middle part of the study area.

3.2.4 Precipitation

The mean precipitation showed similar distribution trends (Figs.7a – e) in December 2013 – 2017. In the north, the mean precipitation was generally low. High mean precipitation values existed in the central equatorial Pacific and extended northwest along the equator. However, in December 2015, although high mean precipitation values were also located in the central equatorial Pacific with a similar trend toward the northwest, a remarkable decrease in mean precipitation occurred that cannot be ignored. In addition, it is important to note that the relatively high-precipitation areas off the coast of Mindanao Island in the other four years turned completely into low-precipitation areas in December 2015.

3.2.5 Surface Chl-*a* concentration

In December 2013 – 2017, high surface Chl-*a* concentrations were pervasive along the shore of Mindanao Island and throughout the MD region (Figs.8a – e). The high value zones to the southeast of the Philippines seemed to extend toward the northeast first and then gradually extended eastward. In contrast, large portions of the northeastern study area were dominated by low surface Chl-*a* concentrations. Overall, the surface Chl-*a* concentrations observed in the MD region in December 2015 slightly increased relative to the values in the other four years.

3.2.6 Wind stress curl

From August to December in 2013 – 2016, the averaged WSCs throughout the study area fluctuated irregularly at first, then they began to exhibit stable positive values after October (Fig.9). And the values of the averaged WSCs in these four years were similar.

3.3 Statistical Analysis of Different Oceanic Data in the MD Region

The area bounded by 2˚ – 12˚N and 125˚ – 150˚E was selected to represent the cold upwelling zone (yellow rectangle in Fig.1). Statistical results of the temperature and salinity at standard depths in this upwelling zone further confirmed the enhanced upwelling strength in December 2015 (Figs.10a and b). Compared with the same layer in the other four years, the average temperatures in December 2015 showed an obvious reduction, especially in the subsurface water (50 – 200 m). Moreover, the reinforced uplift of the subsurface fresh NPIW by this enhanced upwelling caused the decrease of average salinities in the subsurface layer.

Observations also reveal an immense discrepancy in the eco-hydro-climatic conditions within the MD region in December 2015 compared with those in December 2013, 2014, 2016, and 2017, and the statistical results demonstrate that the MD region exhibited an obviously negative MSLA, a lower heat content, relatively low precipitation, higher surface Chl-*a* concentrations in December 2015 (Fig.11) than in the other four years.

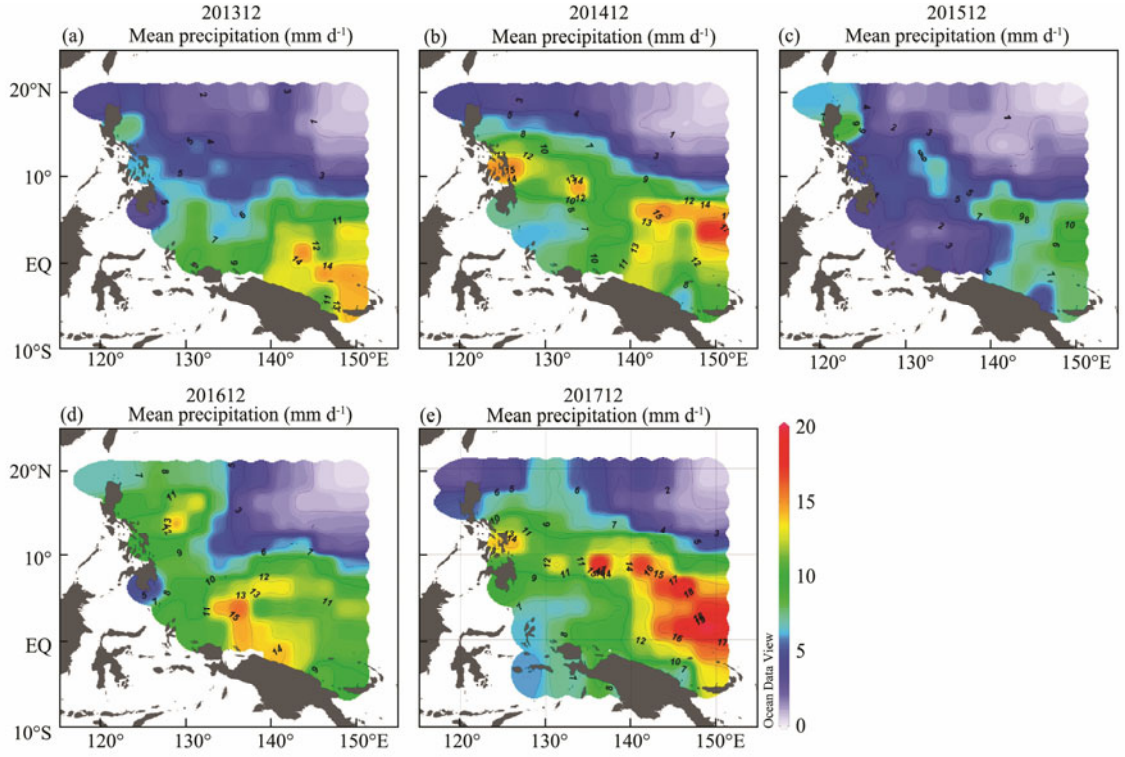

Fig.7 The distributions of the mean precipitation in December 2013 – 2017.

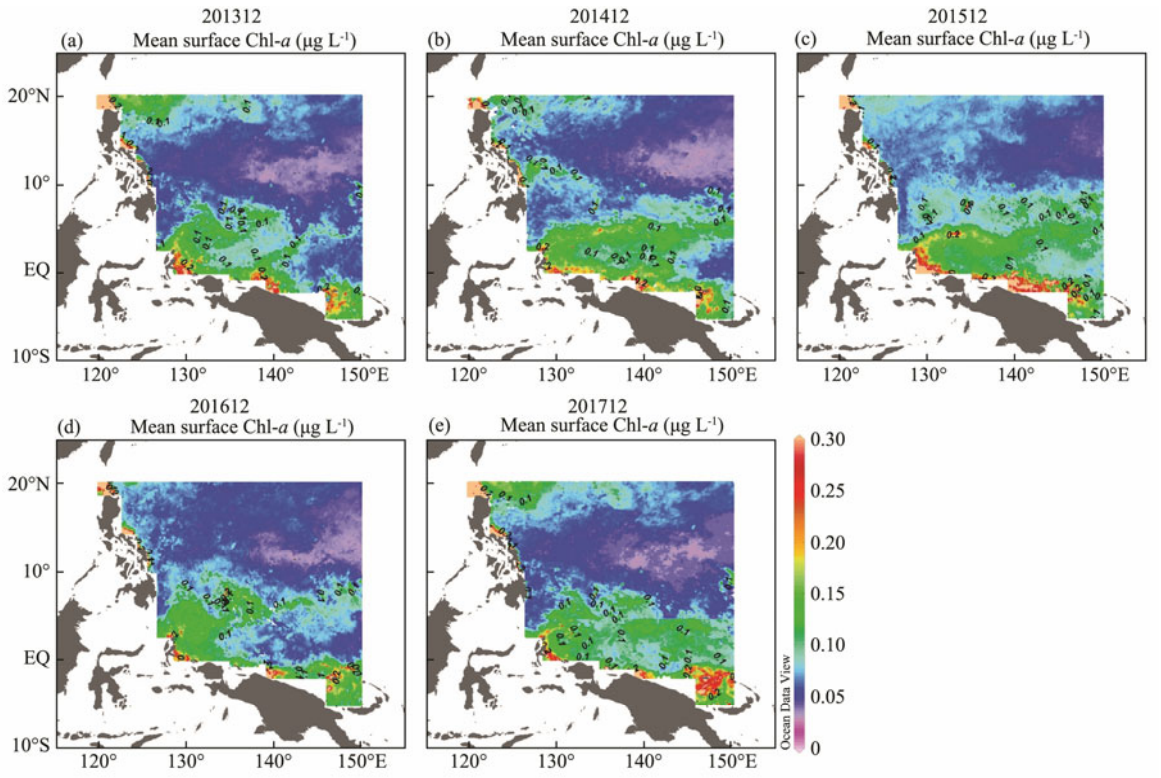

Fig.8 The distributions of the mean surface Chl-*a* concentrations in December 2013–2017.

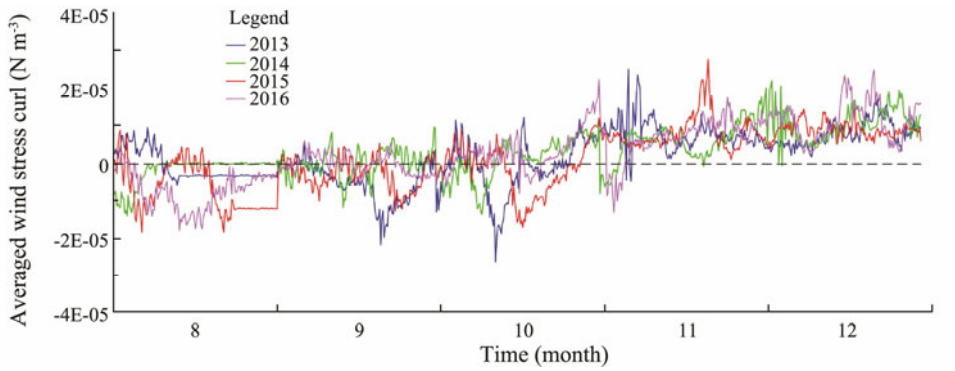

Fig.9 Averaged wind stress curl (WSC) data for the MD region (2°–12°N, 125°–150°E) from August to December in 2013, 2014, 2015 and 2016. Data in the database for 2017 and beyond has not been updated.

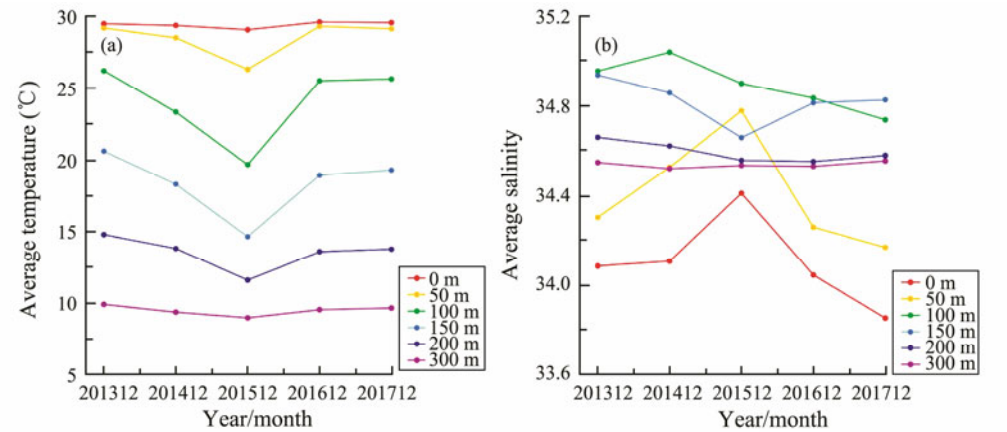

Fig.10 The average temperatures (a) and average salinities (b) at standard depths (0 m, 50 m, 100 m, 150 m, 200 m, and 300 m) in the cold upwelling zone (represented by the yellow rectangle in Fig.1) within the Mindanao Dome region in December 2013–2017.

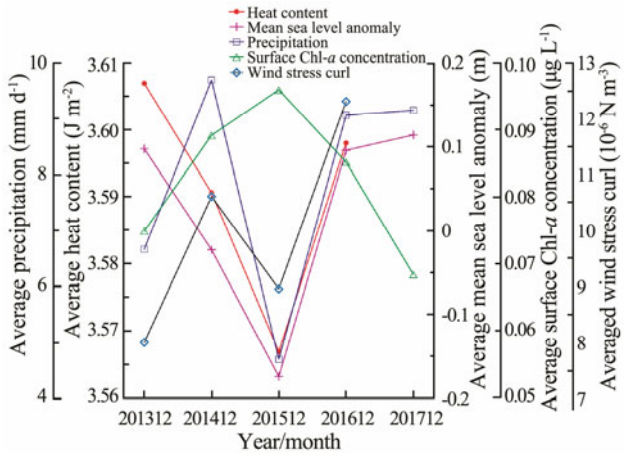

Fig.11 Monthly averages of the heat content, sea level anomaly, precipitation, surface Chl-*a* concentration and wind stress curl in the cold upwelling zone for each December during 2013–2017.

4 Discussion

In 2013, which was a non-El Niño year, the wind-induced NEC transports equatorial surface warm water to the western Pacific; this process not only results in the highest open-ocean water temperatures in the world, *i.e.*, the WPWP (Yan *et al.*, 1992), but also greatly raises the local sea level, generating the positive MSLA over a large area in the western Pacific. The deep convective systems in the WPWP transfer both heat and moisture from the ocean into the atmosphere; hence, the WPWP is a major heat and water vapor source for large-scale atmospheric circulations (Webster and Lukas, 1992; Waliser and Graham, 1993). The warm waters of the WPWP can release considerable latent heat and lead to deep convection and heavy rainfall, more than 2–3 m per year (Delcroix, 1998; Chen *et al.*, 2004).

The associated upward movement of the deep cold water cooled the surface water in the eastern Pacific, while calm winds prevailed in the western equatorial Pacific. Surrounding the Philippines, the westward-flowing NEC, the southward-flowing MC and the eastward-flowing NECC form a highly variable current system, linked to a stable, cold, cyclonic circulation, *i.e.*, the MD. The MD upwelling system just locates in the western part of WPWP. Because of high precipitation rate, which is associated with the warm surface water in this region, the MD region represents a 'warm/rainy/fresh' pool, characterized by large-scale positive SSTA and negative sea surface salinity anomaly (SSSA) in the western Pacific (Figs.12b–d and 13 left). The upwelling induced in the center of the MD uplifts deep cold water and shoals the pycnocline to some extent. The upward movement of this subsurface nutrient-laden water into the euphotic zone helps provide suitable conditions for primary production (Cushing, 1971; Wooster, 1981; Rodier *et al.*, 2000). Thus, relative to its adjacent waters, the MD region tends to exhibit high surface Chl-*a* concentrations (Fig.8).

In early 2014, a strong El Niño was predicted, but it failed to develop due to many factors, such as the absence of sustained eastward winds and currents in the equatorial Pacific (Menkes *et al.*, 2014; McPhaden, 2015). Subsequently, due to a series of westerly wind events (WWEs) in the western equatorial Pacific, a strengthened eastward-flowing NECC occurred (Fig.4c). El Niño signals regenerated in mid-2015 and eventually grew into a super El Niño event, *i.e.*, the 2015/2016 super El Niño event (Chen *et al.*, 2017; Timmermann *et al.*, 2018). The stochastic wind forcing related to this process triggered the downwelling of oceanic Kelvin waves (McPhaden, 1999), sequentially reducing the upwelling of cold subsurface waters in the eastern Pacific cold tongue and leading to surface warming in the central and eastern Pacific (Figs.12e–h). The positive SSTA shifted the atmospheric convection from the western Pacific to the central equatorial Pacific, causing the reduction in equatorial trade winds, which in turn intensified surface warming through the positive Bjerknes feedback in the central equatorial Pacific.

In December 2015, when the 2015/2016 super El Niño event reached its mature phase (Iskandar *et al.*, 2017, Santoso *et al.*, 2017), WWEs strengthened the eastward-flowing NECC (Figs.4c and 13 right), blowing the local surface warm waters, initially within the MD region, into the central and even the eastern Pacific. At the same time, the reflection of upwelling Rossby waves and large easterly wind anomalies at the western boundary happened (Boulanger *et al.*, 2004), contributing to the termination of the El Niño event. In addition, as shown in Fig.9, the averaged WSCs of the MD region began to exhibit stable positive values after October from 2013 to 2016. However, the values of the averaged WSC in December 2015 is not far from those in the other three years. It suggests that though the local Ekman upwelling induced by the positive wind stress curl that has been demonstrated to be the key factor influencing the formation of the MD (Tozuka *et al.*, 2002; Suzuki *et al.*, 2005), it maybe not the key reason for the enhancement of the upwelling in the MD region. Massive loss of surface water and strengthened upwelling Rossby waves together induced the considerable uplift of deep waters in the western Pacific, thus leading to the enhanced upwelling in the MD region in December 2015, as demonstrated in the above analysis of the thermohaline structure variations within the MD region (Figs.2 and 3). Udarbe-Walker and Villanoy (2001) ever revealed that an obvious cold temperature anomaly in the MD region exists at a depth of approximately 100 m and is present in all seasons but reaches a maximum size during winter. However, in December 2015, the upwelling in the MD region was greatly enhanced, which was characterized by the doming of isotherms up to depths of 50 m or even shallower (Fig.2).

Meanwhile, this migration of surface warm water also contributed to the enhancing upwelling of subsurface cold water to the surface layer, accompanied by a series of obvious eco-hydro-climatic changes in the MD region in December 2015 (Figs.4–8). It took away massive amounts of heat and water vapor from the western Pacific and changed the central and eastern Pacific into a new warm/rainy/fresh pool with positive SSTA and negative SSSA (Figs.12f–h). The MD region became into a relatively 'cold/dry/salty'

pool with negative SSTA and positive SSSA (Figs.12f–h and 13 right).

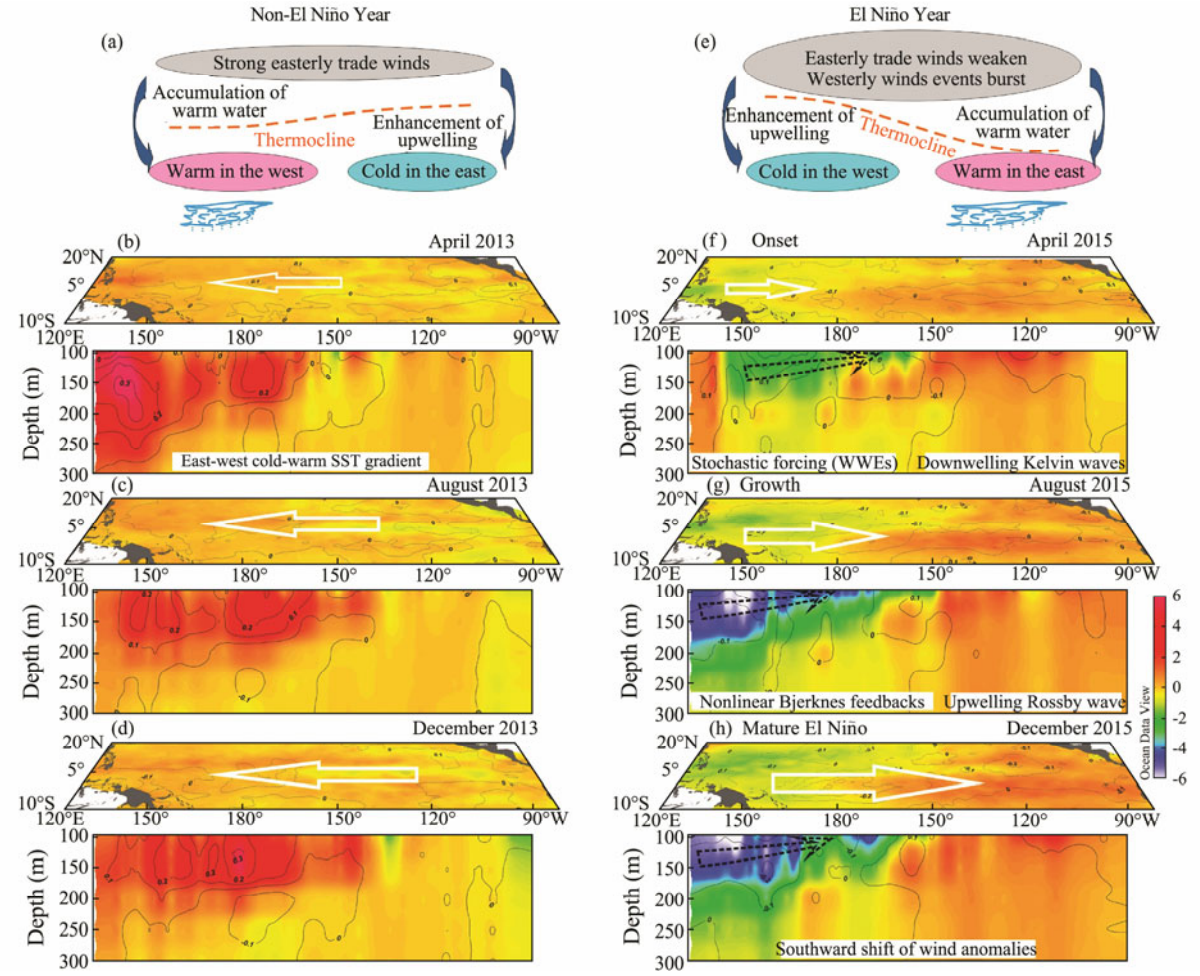

Fig.12 Composite evolution of the sea surface temperature anomalies and subsurface temperature anomalies along the 7˚N in the tropical Pacific in a non-El Niño year (a – d, using 2013 as an example) and an El Niño year (e – h, using 2015 as an example) superposed with salinity anomalies (black contours). The solid white arrows represent wind anomalies, and the dashed black arrows represent the upwelling of cold subsurface waters.

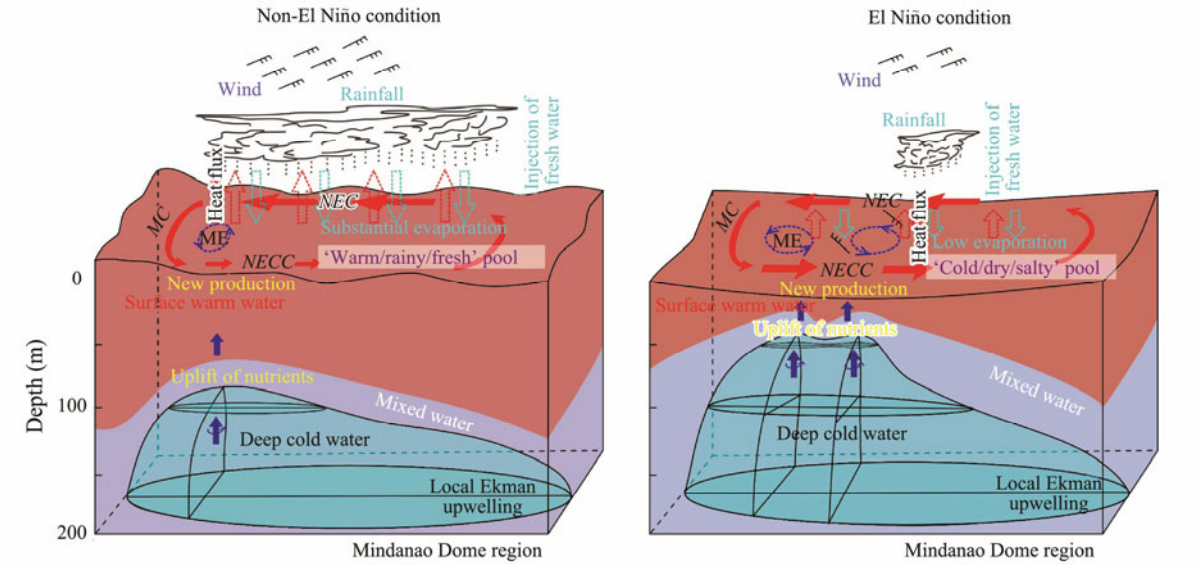

Fig.13 Schematic diagram of the complex processes in the Mindanao Dome region indicating the relationship between the enhanced upwelling and the hydroclimatic variations under normal condition (left) and El Niño condition (right). NEC, North Equatorial Current; KC, Kuroshio Current; MC, Mindanao Current; NECC, North Equatorial Countercurrent; ME, Mindanao eddy.

In addition, the enhanced upwelling served to uplift waters from a deeper layer to a much shallower depth, which not only changed the thermohaline structure but also gradually influenced related hydroclimatic features. A significant reduction in the heat content was the most direct consequence. The consequent reduction in precipitation greatly decreased the fresh water injecting into the MD region, especially in the areas close to the passage connecting the Pacific to the Seas of Indonesia, which presented as a large body of hyperhaline water (Figs.3a-3, b-3, c-3, d-3, e-3, f-3, and g-3). Note that the enhanced upwelling in the MD region was capable of supplying waters with more nutrients to the surface to some extent, and the surface Chl-*a* concentrations also increased in December 2015. Furthermore, the eastward migration of surface warm water also resulted in the notably negative MSLA in the MD region, leading to the enhanced uplift of deep cold water, which produced positive feedbacks in the evolution of this super El Niño event by cooling the western Pacific seawater. Here, the complex processes, by which the enhanced upwelling was linked to the eco-hydro-climatic variations throughout the MD region during the studied El Niño event, were shown in Fig.13.

5 Conclusions

According to Argo-based observations and satellite-based data acquired in December 2013–2017, this paper revealed the complex processes by which the enhanced upwelling was linked to related eco-hydro-climatic variations during the mature phase of the 2015/2016 super El Niño event in the MD region. When this super El Niño event occurred, strong WWEs drove surface warm water migrate from west to east in the equatorial Pacific, producing the negative sea level anomalies and the more active state of subsurface cold water in the tropical western Pacific. The physical reasons of enhancement of the upwelling in the MD region can be attributed to the combination of various factors such as the upwelling Rossby waves and massive loss of surface water. This enhanced upwelling not only cooled and dried the MD region, but also nourished the shallow water and increased the surface Chl-*a* concentrations. It highlights the important role of the El Niño played in local ecology effects and hydro-climatic changes, which is crucial for understanding the interaction between the ocean carbon cycle and local/global climate changes.

Acknowledgements

This work was financially supported by the Strategic Priority Research Program of the Chinese Academy of Sciences (Nos. XDB42010203, XDA19060401), the Science & Technology Basic Resources Investigation Program of China (No. 2017FY100802), the Open fund for Key Laboratory of Marine Geology and Environment, Chinese Academy of Sciences (No. MGE2019KG03), and Post-Doctoral Program in Qingdao in 2019 (No. Y9KY161). The authors gratefully acknowledge the IPRC/APDRC and AVISO+ for providing the Argo-based data and satellite-based products.

References

Boulanger, J. P., Menkes, C., and Lengaigne, M., 2004. Role of high- and low-frequency winds and wave reflection in the onset, growth and termination of the 1997–1998 El Niño. *Climate Dynamics*, **22** (2-3): 267-280.

Chen, G., Fang, C., Zhang, C., and Chen, Y., 2004. Observing the coupling effect between warm pool and 'rain pool' in the Pacific Ocean. *Remote Sensing Environment*, **91** (2): 153-159.

Chen, L. J., Jia, Y. L., and Liu, Q. Y., 2015. Mesoscale eddies in the Mindanao Dome region. *Journal of Oceanography*, **71** (1): 133-140.

Chen, L., Li, T., Wang, B., and Wang, L., 2017. Formation mechanism for 2015/16 super El Niño. *Scientific Reports*, **7**: 2975.

Cravatte, S., Delcroix, T., Zhang, D., McPhaden, M., and Leloup, J., 2009. Observed freshening and warming of the Western Pacific Warm Pool. *Climate Dynamics*, **33** (4): 565-589.

Cushing, D. H., 1971. Upwelling and the production of fish. *Advance in Marine Biology*, **9** (9): 255-300.

Delcroix, T., 1998. Observed surface oceanic and atmospheric variability in the tropical Pacific at seasonal and ENSO timescales: A tentative overview. *Journal of Geophysical Research: Oceans*, **103** (C9): 18611-18633.

Gruber, N., Lachkar, Z., Frenzel, H., Marchesiello, P., and Plattner, G. K., 2011. Eddy-induced reduction of biological production in eastern boundary upwelling systems. *Nature Geoscience*, **4**: 787-792.

Hu, D., Wu, L., Cai, W., Gupta, A. S., Ganachaud, A., Qiu, B., *et al*., 2015. Pacific western boundary currents and their roles in climate. *Nature*, **522** (7556): 299-308.

Iskandar, I., Utari, P. A., Lestari, D. O., Sari, Q. W., Setiabudidaya, D., Khakim, M. Y. N., *et al*., 2017. Evolution of 2015/2016 El Niño and its impact on Indonesia. *American Institute of Physics Conference Proceeding*, **1857** (1): 080001.

Izumo, T., Vialard, J., Lengaigne, M., de Boyer Montegut, C., Behera, S. K., Luo, J. J., *et al*., 2010. Influence of the state of the Indian Ocean Dipole on the following year's El Niño. *Nature Geoscience*, **3** (4): 168-172.

Kashino, Y., Ishida, A., and Hosoda, S., 2011. Observed ocean variability in the Mindanao Dome region. *Journal of Physical Oceanography*, **41** (2): 287-302.

Lengaigne, M., Guilyardi, E., Boulanger, J. P., Menkes, C., Delecluse, P., Inness, P., *et al*., 2007. Triggering of El Niño by westerly wind events in a coupled general circulation model. *Climate Dynamics*, **23** (6): 601-620.

Masumoto, Y., and Yamagata, T., 1991. Response of the western tropical Pacific to the Asian winter monsoon: The generation of the Mindanao Dome. *Journal of Physical Oceanography*, **21**: 1386-1398.

McPhaden, M. J., 1999. Genesis and evolution of the 1997–98 El Niño. *Science*, **283**: 950-954.

Mcphaden, M. J., 2015. Playing hide and seek with El Niño. *Natural Climate Change*, **5** (9): 791-795.

Menkes, C. E., Lengaigne, M., Vialard, J., Puy, M., Marchesiello, P., Cravatte, S., *et al*., 2014. About the role of westerly wind events in the possible development of an El Niño in 2014. *Geophysical Research Letter*, **41** (18): 6476-6483.

O'Connor, B. M., Fine, R. A., Maillet, K. A., and Olson, D. B., 2002. Formation rates of subtropical underwater in the Pacific Ocean. *Deep-Sea Research: Part I*, **49** (9): 1571-1590.

Rodier, M., Eldin, G., and Borgne, R. L., 2000. The western boundary of the equatorial Pacific upwelling: Some consequences of climatic variability on hydrological and planktonic

properties. *Journal of Physical Oceanography*, **56** (4): 463-471.

Rothstein, L. M., Zhang, R. H., Busalacchi, A. J., and Chen, D., 1998. A numerical simulation of the mean water pathways in the subtropical and tropical Pacific Ocean. *Journal of Physical Oceanography*, **28**: 322-343.

Santoso, A., Mcphaden, M. J., and Cai, W. J., 2017. The defining characteristics of ENSO extremes and the strong 2015/2016 super El Niño. *Reviews of Geophysics*, **55**: 1079-1129.

Suga, T., Kato, A., and Hanawa, K., 2000. North Pacific tropical water: Its climatology and temporal changes associated with the climate regime shift in the 1970s. *Progress in Oceanography*, **47** (2): 223-256.

Suzuki, T., Sakamoto, T. T., Nishimura, T., Okada, N., Emori, S., Oka, A., *et al*., 2005. Seasonal cycle of the Mindanao Dome in the CCSR/NIES/FRCGC Atmosphere-Ocean coupled model. *Geophysical Research Letter*, **32** (17): 195-221.

Sydeman, W. J., Garcia-Reyes, M., Schoeman, D. S., Rykaczewski, R. R., Thompson, S. A., Black, B. A., *et al*., 2014. Climate change and wind intensification in coastal upwelling ecosystems. *Science*, **345** (6192): 77-80.

Talley, L., 1993. Distribution and formation of North Pacific intermediate water. *Journal of Physical Oceanography*, **23** (3): 517-538.

Timmermann, A., An, S. I., Kug, J. S., Jin, F. F., and Zhang, X., 2018. El Niño-Southern Oscillation complexity. *Nature*, **559** (7715): 535-545.

Tozuka, T., Kagimoto, T., Masumoto, Y., and Yamagata, T., 2002. Simulated multiscale variations in the western tropical Pacific: The Mindanao Dome revisited. *Journal of Physical Oceanography*, **32** (5): 1338-1359.

Udarbe-Walker, M. J. B., and Villanoy, C. L., 2001. Structure of potential upwelling areas in the Philippines. *Deep-Sea Research Part I*, **48** (6): 1499-1518.

Waliser, D. E., and Graham, N. E., 1993. Convective cloud systems and warm-pool sea surface temperatures: Coupled interactions and self-regulation. *Journal of Geophysical Reseach: Atmosphere*, **98** (D7): 12881-12893.

Webster, P. J., and Lukas, R., 1992. TOGA COARE: The coupled ocean-atmosphere response experiment. *Bulletin of the American Meteorological Society*, **73** (9): 1377-1416.

Wooster, W. S., 1981. An upwelling mythology. In: *Coastal Upwelling*. Richards, F. A., ed., American Geophysical Union, New York, 1-3.

Yan, X. H., Ho, C. R., Zheng, Q., and Klemas, V., 1992. Temperature and size variabilities of the Western Pacific Warm Pool. *Science*, **258** (5088): 1643-1645.

Zhang, R. H., Tian, F., Busalacchi, A. J., and Wang, X., 2018. Freshwater flux and ocean chlorophyll produce nonlinear feedbacks in the tropical Pacific. *Journal of Climate*, **32**: 2037-2055.

Zhang, R. H., Tian, H., Zhi, F. H., and Kang, X. B., 2019. Observed structural relationships between ocean chlorophyll variability and its heating effects on the ENSO. *Climate Dynamics*, **53**: 5165-5186.

Zhao, J., Li, Y., and Wang, F., 2013. The role of Mindanao Dome in the variability of the Pacific North Equatorial Current bifurcation. *Journal of Oceanography*, **69** (3): 313-327.

(Edited by Chen Wenwen)